



Available online at www.sciencedirect.com



Journal of Molecular Spectroscopy xxx (2007) xxx–xxx

Journal of
MOLECULAR
SPECTROSCOPY

www.elsevier.com/locate/jms

Resonant two-photon ionization and mass-analyzed threshold ionization spectroscopy of the selected rotamers of *m*-methoxyaniline and *o*-methoxyaniline

Jung Lee Lin^a, Chen-Jso Huang^{a,b}, Cheng-Huang Lin^b, Wen Bih Tzeng^{a,*}^a Institute of Atomic and Molecular Sciences, Academia Sinica, P.O. Box 23-166, 1, Section 4, Roosevelt Road, Taipei 10617, Taiwan^b Department of Chemistry, National Taiwan Normal University, 88, Section 4, Roosevelt Road, Taipei 11677, Taiwan

Received 20 March 2007

Abstract

We report the resonant two-photon ionization and mass-analyzed threshold ionization (MATI) spectra of *m*-methoxyaniline and *o*-methoxyaniline. The vibronic features of *m*-methoxyaniline are built on 34308 ± 2 and 34495 ± 2 cm^{-1} corresponding to the origins of the $S_1 \leftarrow S_0$ electronic transition (E_1 's) of the *cis* and *trans* rotamers. Analysis of the MATI spectra gives the adiabatic ionization energies (IEs) of 59983 ± 5 and 60879 ± 5 cm^{-1} for these two species. *o*-Methoxyaniline is found to have only one stable structure whose E_1 and IE are 33875 ± 2 and 58678 ± 5 cm^{-1} , respectively. Most of the active vibrations of *m*- and *o*-methoxyaniline in the electronically excited S_1 and cationic ground D_0 states result from the in-plane ring vibrations. Comparing these data with those of *p*-methoxyaniline allows us to learn about the vicinal substitution effects resulting from the relative locations of the NH_2 and OCH_3 substituents.

© 2007 Published by Elsevier Inc.

Keywords: Resonant two-photon ionization; Threshold ionization; Vibronic spectra; Cation spectra; *m*-Methoxyaniline; *o*-Methoxyaniline

1. Introduction

Investigations on molecular conformers are essential for understanding many biochemical phenomena and processes [1]. *m*-Methoxyaniline can form a conducting copolymer with diphenylamine and may be used in many industrial applications [2]. The ionization energy (IE) of *m*-methoxyaniline has been reported on the basis of the electron impact ionization experiments [3]. However, the conformation of this species is not specified. Up to date, the detailed spectroscopic data of *m*-methoxyaniline in the electronically excited S_1 and cationic ground D_0 states are still not available in the literature. Previous studies [4,5] show that many *meta* di-substituted benzenes may possess *cis* and *trans* rotational conformers (rotamers). These rota-

mers may coexist in a chemical sample. Since the origins of the electronic transitions of these rotamers may only differ by a few tens to a few hundreds of wavenumbers, the resulting vibronic features may overlap in a common spectral region. To study the selected rotamers, it requires a high-resolution spectroscopic method. Supersonic jet-cooled resonance-enhanced multiphoton ionization (REMPI) in conjunction with time-of-flight mass spectrometry (TOFMS) and hole-burning spectroscopy are useful techniques to confirm the presence of different conformers [5,6]. These methods can provide information about the molecular vibrations of specific conformers in the electronically excited state.

An alternative approach to study molecular conformers is to utilize zero-kinetic energy (ZEKE) photoelectron or mass-analyzed threshold ionization (MATI) spectroscopy with two-color resonant excitation scheme. Both methods can give precise adiabatic IEs of the selected conformers as well as the active vibrations of the corresponding cations

* Corresponding author. Fax: +886 2 23620200.
E-mail address: wbt@sinica.edu.tw (W.B. Tzeng).

[4,7]. Since the MATI technique detects ZEKE ions, it has an additional advantage of providing mass information, it has an additional advantage of providing mass information. Thus, it is suitable for the spectroscopic studies of systems containing radicals [8], isotopomers [9], complexes [10], and impurities [11].

When the two substituents of a di-substituted benzene locate in *ortho* position, existence of possible rotamers can be related to the nature, intra-molecular interaction and steric hindrance of the substituents. Previous studies indicate that only one stable structure exists for catechol [12], *o*-fluorophenol [13], and *o*-methoxyphenol [13]. Intuitively, one would expect that *o*-methoxyaniline also has only one stable structure. However, experimental and theoretical evidences are needed. The IE of this molecule has been determined by the charge transfer experiments [14]. To the best of our knowledge, little is known about the spectroscopic properties of *o*-methoxyaniline in the S_1 and D_0 states.

In this paper, we report the one-color, two-color resonant two-photon ionization (1C, 2C-R2PI) and MATI spectra of *m*-methoxyaniline and *o*-methoxyaniline. These new experimental data provide information about the origins of the $S_1 \leftarrow S_0$ electronic transition (E_1 's), IEs, and vibrations of the selected rotamers in the electronically excited S_1 and cationic ground D_0 states. We have also performed ab initio and density functional theory (DFT) calculations to support our experimental findings. The computed vibrational frequencies are used to assign the obtained vibronic and MATI spectra. Comparing these data with those of *p*-methoxyaniline [15,16] helps us to gain knowledge about the vicinal substitution effect on substituted anilines.

2. Experimental and computational methods

The experiments were performed with a TOF mass spectrometer described elsewhere [7]. Both *m*-methoxyaniline (99% purity) and *o*-methoxyaniline (99% purity) were purchased from Sigma–Aldrich and used without further purification. The vapor of these liquid samples was seeded into 2–3 bar of helium and expanded into the vacuum through a pulsed valve with a 0.15 mm diameter orifice. The two-color resonant two-photon excitation process was initiated by utilizing two independent tunable UV laser systems controlled by a delay/pulse generator (Stanford Research Systems DG535). The excitation source is a Nd:YAG pumped dye laser (Quanta-Ray PRO-190-10/Lambda-Physik, ScanmateUV with BBO-III crystal; Rhodamine 575, 590, 610, and 640 dyes) with bandwidth $\leq 0.3 \text{ cm}^{-1}$. The visible radiation is frequency doubled to produce UV radiation. The ionization UV laser (Lambda-Physik, ScanmateUV with BBO-III crystal; LDS 765, and 821 dyes) was pumped by a frequency-doubled Nd:YAG laser (Continuum Surelite I-10). A Fizeau-type wavemeter (New Focus 7711) was used to calibrate the wavelengths of both lasers. These two counter-propagating laser beams were focused and inter-

sected perpendicularly with the molecular beam at 50 mm downstream from the nozzle orifice.

In the MATI experiments, the pump laser was used to excite the selected molecular species to a specific vibronic level in the S_1 state. The probe laser was scanned to bring the electronically excited molecule to high n Rydberg states lying a few wavenumbers below the ionization limit. Under this condition, both prompt ions and Rydberg neutrals were formed simultaneously in the laser and molecular beam interaction zone. A pulsed electric field of -1.0 V/cm was switched on about 190 ns after the occurrence of the laser pulses to reject the prompt ions. About $9.60 \mu\text{s}$ later, a second pulsed electric field of $+200 \text{ V/cm}$ was applied to field-ionize the Rydberg neutrals. These threshold ions were then accelerated and passed through a field-free region before being detected by a dual-stacked micro-channel plate detector.

We have also performed ab initio and density functional theory (DFT) calculations to support our experimental findings. All calculations were performed by using the GAUSSIAN 03 program package [17]. The restricted Hartree–Fock (RHF), configuration interaction singles (CIS), and unrestricted HF (UHF) calculations with the 6-311++G** basis set were applied to predict the molecular properties including the vibrational frequencies of these molecules in the S_0 , S_1 , and D_0 states, respectively. The IE was obtained as the difference in the zero-point level (ZPL) energies of the molecules in the S_0 and D_0 states. The computed vibrational frequencies are used to assign the obtained vibronic and MATI spectra.

3. Results

3.1. *m*-Methoxyaniline

3.1.1. 1C-R2PI spectrum of *m*-methoxyaniline

The E_1 's of *p*-aminophenol, *cis m*-aminophenol, and *trans m*-aminophenol, and *p*-methoxyaniline have been reported to be 31393, 34110, 34468, and 31581 cm^{-1} , respectively [4,15,16,18–20]. This information helps us to set a proper range for scanning our laser to locate the E_1 of *m*-methoxyaniline. Fig. 1 shows the 1C-R2PI spectrum of *m*-methoxyaniline in the energy range near its $S_1 \leftarrow S_0$ electronic transition. Similar to that reported previously for *cis* and *trans m*-aminophenol [18–20], the vibronic bands appear in two series which are built on 34308 ± 2 and $34495 \pm 2 \text{ cm}^{-1}$ corresponding to the transition origins of the *cis* and *trans* rotamers of *m*-methoxyaniline, respectively. We have applied both ab initio and DFT calculations to predict the E_1 's of these two rotamers. The ZPLs in the S_0 and S_1 states were calculated by using the RHF and CIS methods with the 6-311++G** basis set, respectively. The E_1 's of *cis* and *trans m*-methoxyaniline are estimated to be 40605 and 41800 cm^{-1} , respectively. With the same basis set, the time-dependent Becke three-parameter functional with the PW91 correlation functional (TD-B3PW91) method gives 33612 and 35371 cm^{-1} for

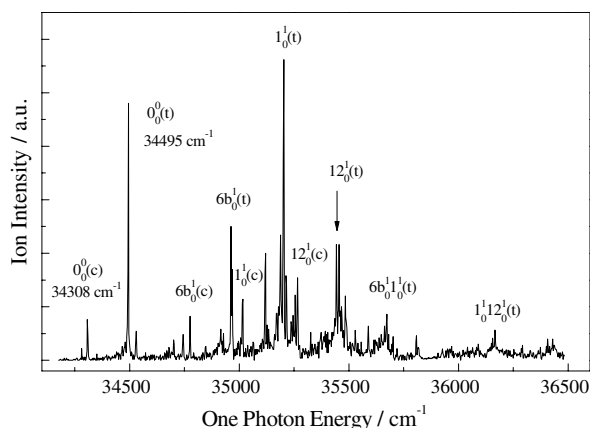


Fig. 1. 1C-R2PI spectrum of *m*-methoxyaniline (*c* = *cis*, *t* = *trans*).

these two corresponding species. Although the calculated results slightly deviate from the measured ones, both methods predict that the *trans* has a slightly higher E_1 than the *cis* rotamer of *m*-methoxyaniline. Thus, the theoretical calculations support our assignment for the band origins of these two rotamers. Similar findings have been reported for *m*-aminophenol [19] and *m*-cresol [21].

To assign the vibronic spectral features, we compare the measured frequencies of *m*-methoxyaniline with the available experimental data for *m*-aminophenol [4,18,19] and *p*-methoxyaniline [15,16] in the S_1 state and those for some aniline derivatives [22] in the S_0 state as well as conformity with our calculated results for the S_0 , S_1 , and D_0 states. The observed bands associated with excitation photon energies, relative intensities, shifts from the origins, and possible assignments are listed in Table 1, along with the calculated vibrational frequencies. The pronounced bands resulting

Table 1
Observed bands in the 1C-R2PI spectrum of *m*-methoxyaniline and possible assignments

Energy (cm ⁻¹)	Relative intensity	Shift (cm ⁻¹)	Cal. ^a (cm ⁻¹)	Assignment ^b
<i>cis</i>				
34308	100	0		0_0^0
34530	71	220	206	τ , CH ₃ torsion
34775	108	465	507	$6b_1^1$, β (CCC)
35016	150	706	707	1_1^1 , breathing
35266	203	956	947	12_1^1 , β (CCC)
<i>trans</i>				
34495	100	0		0_0^0
34744	10	249	249	τ , CH ₃ torsion
34963	52	468	503	$6b_1^1$, β (CCC)
35120	42	625	649	4_1^1 , γ (CCC)
35204	117	709	702	1_1^1 , breathing
35443	45	948		$1_1^1 \tau$
35456	45	961	948	12_1^1 , β (CCC)
35674	18	1179		$6b_1^1 1_1^1$
36166	12	1671		$1_1^1 12_1^1$

^a Obtained from the CIS/6-311++G** calculations (scaled by 0.9).

^b β , in-plane bending, γ , out-of-plane bending.

from the $6b_1^1$, 1_1^1 , and 12_1^1 transitions appear at 465, 706, and 956 cm⁻¹ for the *cis* rotamer and at 468, 709, and 961 cm⁻¹ for the *trans* rotamer, respectively. The present results indicate that different orientation of the OCH₃ with respect to the NH₂ group only slightly affects the frequencies of these in-plane ring deformation vibrations.

3.1.2. 2C-R2PI and MATI spectra of *cis m*-methoxyaniline

The IE of *m*-methoxyaniline is reported to be 7.8 ± 0.1 eV on the basis of the electron impact ionization measurement [3]. Since this technique typically utilizes electron energy of about 70 eV, it may give information about the vertical IE rather than the adiabatic IE. Due to lack of energy resolution, it does not provide information about molecular conformation. Here, we performed the 2C-R2PI and MATI experiments to determine the adiabatic IEs of the selected species with high precision. Fig. 2a displays the photoionization efficiency (PIE) curve of *cis m*-methoxyaniline recorded by ionizing via its $S_1 0^+$ intermediate level at 34308 cm⁻¹. Investigation on the rising step gives an IE of 59991 ± 10 cm⁻¹. Since the MATI technique involves detection of threshold ions resulting from pulsed field ionization, it leads to a sharp peak at the ionization threshold and yields a more definitive IE value, as seen in Fig. 2b. Analysis on the 0^+ band gives the field-corrected IE to be 59983 ± 5 cm⁻¹ (7.4369 ± 0.0006 eV). The distinct MATI feature shifted from the 0^+ band by 726 cm⁻¹ results from the 1^1 vibration of the *cis m*-methoxyaniline cation in

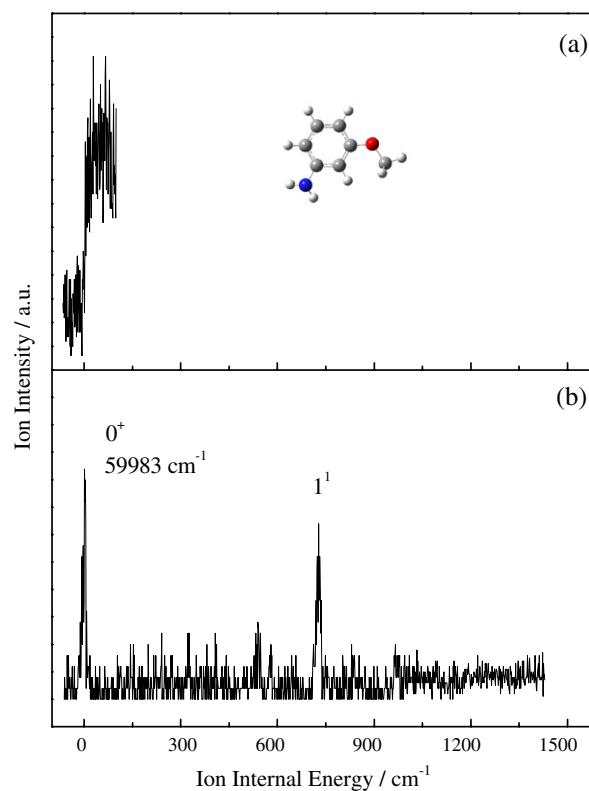


Fig. 2. (a) PIE curve, (b) MATI spectrum of *cis m*-methoxyaniline recorded by ionizing via the $S_1 0^+$ state.

the D_0 state. It is noted that the frequency of this breathing vibration of the *cis m*-aminophenol cation was found to be 744 cm^{-1} [19].

3.1.3. 2C-R2PI and MATI spectra of *trans m*-methoxyaniline

Fig. 3a shows the PIE curve of *trans m*-methoxyaniline obtained by ionizing via the $S_1 0^0$ intermediate state at 34495 cm^{-1} , giving an IE value of $60880 \pm 10\text{ cm}^{-1}$. Fig. 3b–d show the MATI spectra of *trans m*-methoxyaniline recorded by ionizing via the 0^0 , $6b^1(0^0 + 468\text{ cm}^{-1})$, and $1^1(0^0 + 709\text{ cm}^{-1})$ levels in the S_1 state. These yield the field-corrected IE of $60879 \pm 5\text{ cm}^{-1}$ ($7.5480 \pm 0.0006\text{ eV}$). The pronounced bands at 507, 724, and 974 cm^{-1} result from the in-plane ring deformations $6b$, 1 , and 12 of the *trans m*-methoxyaniline cation. The respective frequencies of these in-plane vibrations are measured to be 479, 735, and 985 cm^{-1} for the *trans m*-aminophenol cation [19]. The band at 696 cm^{-1} in Fig. 3d is tentatively assigned to the combination of the $6a$ vibration and the O–CH₃ torsion of the *trans m*-methoxyaniline cation. The weak band at 1449 cm^{-1} results from the overtone vibration 1^2 .

3.2. *o*-Methoxyaniline

3.2.1. 1C-R2PI spectrum of *o*-methoxyaniline

Fig. 4 displays the 1C-R2PI spectrum of *o*-methoxyaniline in the energy range near its $S_1 \leftarrow S_0$ electronic transi-

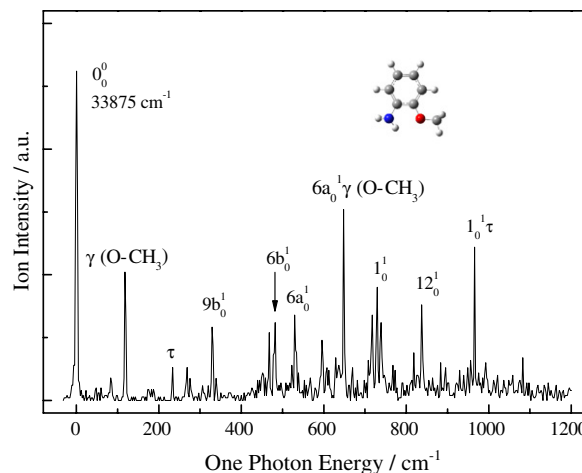


Fig. 4. 1C-R2PI spectrum of *o*-methoxyaniline.

tion. The band origin appears at $33875 \pm 2\text{ cm}^{-1}$. Similar to *o*-fluorophenol and *o*-methoxyphenol [13], only one stable structure is found for *o*-methoxyaniline. Table 2 lists the observed vibronic bands and their possible assignments. The strong vibronic bands at 118 and 648 cm^{-1} are related to the out-of-plane O–CH₃ bending (designated as $\gamma(\text{O-CH}_3)$) and its combination with the in-plane ring deformation $6a$. The moderately intense bands at 482, 529, 729, and 838 cm^{-1} result from the $6a$, $6a$, 1 , and 12 transitions of *o*-methoxyaniline. The corresponding frequencies of vibrations $6a$, 1 , and 12 of *o*-methoxyphenol in the S_1 state are reported to be 526, 726, and 814 cm^{-1} , respectively [13].

3.2.2. 2C-R2PI and MATI spectra of *o*-methoxyaniline

Fig. 5a shows the PIE curve of *o*-methoxyaniline obtained by ionizing via the $S_1 0^0$ intermediate state at 33875 cm^{-1} . This gives an IE value of $58684 \pm 10\text{ cm}^{-1}$.

Table 2

Observed bands in the 1C-R2PI spectrum of *o*-methoxyaniline and possible assignments

Energy (cm ⁻¹)	Relative intensity	Shift (cm ⁻¹)	Cal. ^a (cm ⁻¹)	Assignment ^b
33875	100	0		0^0 , band origin
33993	39	118	98	$\gamma(\text{O-CH}_3)$
34109	10	234	210	τ , CH ₃ torsion
34144	10	269	282	$10a^1_0$, $\gamma(\text{C-OCH}_3, \text{C-NH}_2)$
34204	22	329	329	$9a^1_0$, $\beta(\text{CCC})$
34343	21	468	462	$16a^1_0$, $\gamma(\text{CCC})$
34357	24	482	463	$6a^1_0$, $\beta(\text{CCC})$
34404	26	529	561	$6a^1_0$, $\beta(\text{CCC})$
34471	18	596		$9a^1_0$, $10a^1_0$
34523	58	648		$6a^1_0$, $\gamma(\text{O-CH}_3)$
34593	26	718		$6a^1_0$, τ
34604	34	729	737	1^1_0 , breathing
34614	24	739		$16a^1_0$, $10a^1_0$
34713	29	838	817	12^1_0 , $\beta(\text{CCC})$
34841	47	966		1^1_0 , τ
34958	13	1083		12^1_0 , τ

^a Obtained from the CIS/6-311++G** calculations (scaled by 0.9).

^b β , in-plane bending, γ , out-of-plane bending.

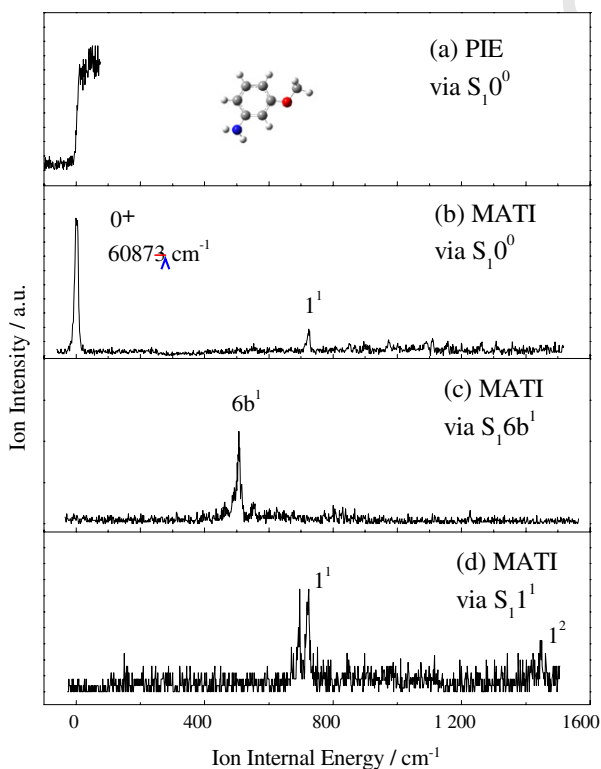


Fig. 3. (a) PIE curve via the 0^0 , (b–d) MATI spectra of *trans m*-methoxyaniline recorded by ionizing via the 0^0 , $6b^1$, and 1^1 levels in the S_1 state, respectively.

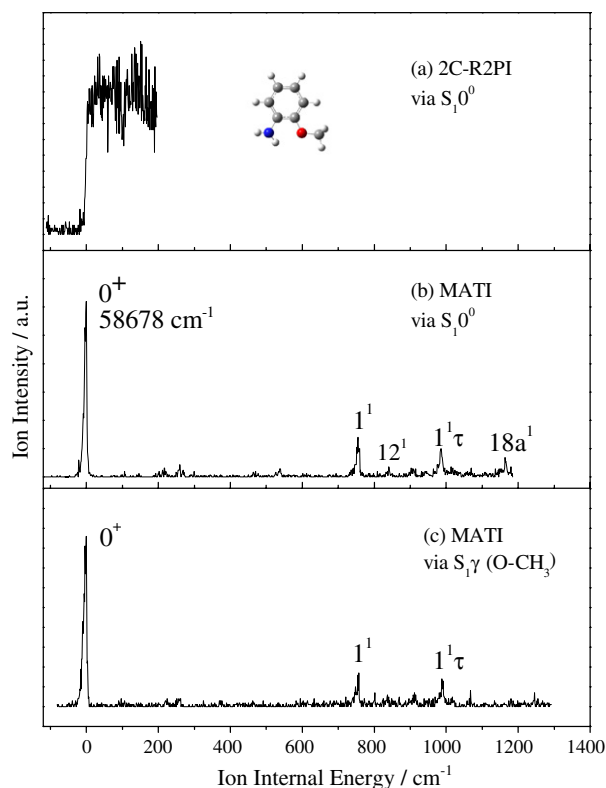


Fig. 5. (a) 2C-R2PI spectrum via the 0^0 , (b and c) MATI spectra of *o*-methoxyaniline recorded by ionizing via the 0^0 and $\gamma(\text{O}-\text{CH}_3)$ levels in the S_1 state, respectively.

Fig. 5b and c display the MATI spectra recorded by ionizing via the 0^0 and $\gamma(\text{O}-\text{CH}_3)$ ($0^0 + 118 \text{ cm}^{-1}$) levels in the S_1 state. The field-corrected adiabatic IE is determined to be $58678 \pm 5 \text{ cm}^{-1}$ ($7.2751 \pm 0.0006 \text{ eV}$), which is slightly lower than the reported value of $7.5 \pm 0.1 \text{ eV}$ on the basis of the charge transfer experiments [14]. The distinct bands at 755 and 838 cm^{-1} result from the in-plane vibrations 1 and 12 of the *o*-methoxyaniline cation in the D_0 state. The corresponding frequencies of the *o*-methoxyphenol cation were found to be 756 and 829 cm^{-1} , respectively [13]. Although the intensity of all other bands in Fig. 5b and c is low, the signal-to-noise ratio is acceptable. The tentative assignments of these weak MATI bands are listed in Table 3.

4. Discussion

4.1. *m*-Methoxyaniline

Our calculations at the B3PW91/6-311++G** level predict that only two stable conformers of *m*-methoxyaniline exist. In the S_0 state the ZPL energies of the *trans* and *cis* rotamers are calculated to be -401.934763 and -401.934283 Hartrees, respectively. In other words, the *trans* lies in an energy level lower than the *cis* rotamer by 105 cm^{-1} . The energy barrier to the internal rotation of the $\text{O}-\text{CH}_3$ group for the *cis-trans* isomerization can be

Table 3
Observed bands (in cm^{-1}) in the MATI spectra of *o*-methoxyaniline^a and possible assignments

Intermediate level		Cal.	Assignment ^b
$S_1 0^0$	$S_1 \tau^1$		
217	224	210	τ , CH_3 torsion
260	261	276	$10a^1$, $\gamma(\text{C}-\text{OCH}_3, \text{C}-\text{NH}_2)$
755	757	751	1^1 , breathing
840	836	857	12^1 , $\beta(\text{CCC})$
988	988		$1^1 \tau$
	1068	1066	$12^1 \tau$
1164		1164	$18a^1$, $\beta(\text{CH})$

^a The experimental values are shifts from 58678 cm^{-1} , whereas the calculated ones (scaled by 0.95) are obtained from the UHF/6-311++G** calculations.

^b ν —stretching, β —in-plane bending, γ —out-of-plane bending.

calculated by using the GAUSSIAN 03 program package [17]. Fig. 6 shows the one-dimensional potential energy surfaces of *m*-methoxyaniline along the dihedral angle of $\text{C}2\text{C}3\text{OC}(\text{H}_3)$. This result predicts that the energy barrier for the *cis-trans* isomerization of *m*-methoxyaniline in the S_0 state is in the range of 1051 – 1100 cm^{-1} . It has been reported that the energy barrier to the $\text{O}-\text{CH}_3$ torsion of *p*-dimethoxybenzene is 712 cm^{-1} at the B3PW91/6-31G* level of calculation [7]. This shows that the NH_2 group in the *meta* position causes a slightly greater the energy barrier to the $\text{O}-\text{CH}_3$ torsion than the OCH_3 group in the *para* position.

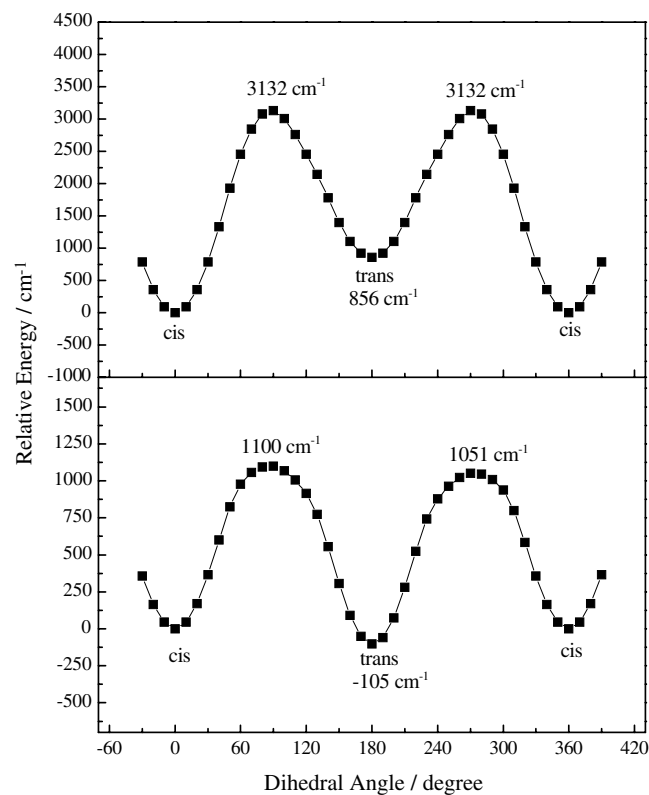


Fig. 6. One-dimensional potential energy surfaces along the dihedral angle of $\text{C}2\text{C}3\text{OC}(\text{H}_3)$ of *m*-methoxyaniline in the (a) D_0 and (b) S_0 states.

The respective E_1 's of the *cis* and *trans* rotamers of *m*-methoxyaniline are found to be 34308 and 34495 cm^{-1} on the basis our 1C-R2PI experiments. Taking into account this energy difference and calculated energies for the two rotamers in the S_0 state, the ZPL in the S_1 state of the *trans* rotamer is expected to be higher than that of the *cis* one by 82 cm^{-1} . This indicates that in the S_1 state the interaction between the NH_2 and OCH_3 groups of the *cis* rotamer is stronger than that of the *trans* rotamer. The adiabatic IEs of the *cis* and *trans* rotamers of *m*-methoxyaniline are determined to be $59983 \pm 5 \text{ cm}^{-1}$ and $60879 \pm 5 \text{ cm}^{-1}$, respectively, with our MATI experiments. With these measured IE values and the calculated energies in the neutral S_0 state, the ZPL in the cationic D_0 state of the *trans* rotamer is deduced to be higher than that of the *cis* rotamer by 791 cm^{-1} . Similar to the argument stated previously for the S_1 state, the interaction between the NH_2 and OH groups of *cis m*-methoxyaniline is stronger than that of *trans m*-methoxyaniline in the cationic D_0 state. Our unrestricted B3PW91/6-311++G** calculations predict that the ZPL of the *trans* rotamer lies higher than that of the *cis* rotamer by 856 cm^{-1} . Although the magnitude is slightly different, the general trend predicted by the theoretical calculations is consistent with the experimental findings. The calculated results shown in Fig. 6 also show that the energy barrier for the *cis*–*trans* isomerization of *m*-methoxyaniline in the D_0 state is 3132 cm^{-1} , which is greater than the value of 1051–1100 cm^{-1} in the S_0 state. Our B3PW91/6-311++G** calculations predict that the C3– OCH_3 bond of *m*-methoxyaniline is about 1.360 Å in the S_0 state and becomes 1.322 Å in the D_0 state. The shortening of this C3– OCH_3 bond implies a stronger chemical bond and hence a greater isomerization energy barrier in the cationic D_0 state. Therefore, the theoretical calculations support our experimental findings. A similar argument has been reported for *m*-aminophenol [19].

Table 4 lists the measured frequencies of in-plane vibrations $6b_A$, 1, and 12 of the *cis* and *trans* rotamers of *m*-methoxyaniline in the S_1 and D_0 states. Frequencies of mode $6b_A$ are measured to be 465 and 537 cm^{-1} for the *cis*, and 468 and 507 cm^{-1} for the *trans* rotamer in the S_1 and D_0 states, respectively. Evidently, the vibrational frequency of the electronically excited S_1 state is less than that of the cationic ground D_0 state. A plausible interpretation is that the molecular geometry is less rigid in the S_1 state than that in the D_0 state. A similar observation has been reported for *p*-methoxyphenol [20] and *p*-methylanisole [23]. Another interesting finding is that frequency of vibra-

Table 4
Frequencies (in cm^{-1}) of some in-plane ring vibrations observed in the vibronic and cation spectra of *m*-methoxyaniline in the S_1 and D_0 states

Vibration	<i>cis</i>		<i>trans</i>	
	S_1	D_0	S_1	D_0
$6b_A$	465	537	468	507
1	706	726	709	724
12	956	—	961	974

tion $6b_A$ of the *cis* is slightly less than that of the *trans* rotamer in the S_1 . However, it is greater than that of the *trans* in the D_0 state. This indicates that different orientation of the OCH_3 group with respect to the NH_2 group as well as the electronic structures can influence the degree of both substituents involved in overall motion. The above argument can also be applied to interpret the observed frequencies of vibrations 1 and 12, as listed in Table 4.

When the $S_1(6b_A^1)$ and $S_1(1^1)$ states were used as the intermediate levels for recording the MATI spectra of *trans m*-methoxyaniline, the results show that all the bands related to the same vibrational pattern exhibit strong intensities, as seen in Fig. 3c and d. This indicates that the geometry and the vibrational coordinates of vibrations $6b_A$ and 1 of the cation resemble those of the neutral species in the S_1 state. A similar finding has been reported for *trans m*-aminophenol [19].

4.2. *o*-Methoxyaniline

To search for possible conformers of *o*-methoxyaniline, we have performed many ab initio and DFT calculations in the S_0 , S_1 , and D_0 states. The initial molecular geometries have configurations with different orientation of the $\text{O}-\text{CH}_3$ with respect to the $\text{O}-\text{H}$ group. As a result, only one stable structure with the $\text{N}-\text{H}\cdots\text{O}-\text{CH}_3$ configuration (see the inserted figure in Fig. 4.) is found. This result is similar to that of *o*-methoxyphenol [13], whose only stable structure has the $\text{O}-\text{H}\cdots\text{O}-\text{CH}_3$ configuration. The general spectral features of *o*-methoxyaniline in Fig. 4 are somewhat similar to those of *o*-methoxyphenol [13]. One expects that the active vibrations of these two species in the S_1 state are alike. The 0^+ bands of the MATI spectra recorded by ionizing through the 0^0 and ($0^0 + 118 \text{ cm}^{-1}$) intermediate levels give the same IE value, as seen in Fig. 5b and c. This indicates that both cation spectra of *o*-methoxyaniline result from the same form. Therefore, our experimental results also imply that there is only one stable structure for *o*-methoxyaniline in the D_0 state.

Analysis on the vibronic and cation spectra of *o*-methoxyaniline shows that frequency of the breathing motion (mode 1) is 729 cm^{-1} in the S_1 and 756 cm^{-1} in the D_0 state. This indicates that the molecular geometry of *o*-methoxyaniline is less rigid in the neutral S_1 state than that in the cationic D_0 state, as in the cases of the *cis* and *trans* rotamers of *m*-methoxyaniline stated previously.

4.3. Substitution effects

The $S_1 \leftarrow S_0$ transition of benzene derivatives is known to undergo an $\pi\pi^*$ electronic excitation, leading to an expansion in the ring [24]. A substituent can interact with the aromatic ring by the inductive effect through the σ bond or by the resonance effect through the π orbitals. The collective effect gives rise to a slight change in the neighboring electron density and molecular geometry. Consequently, the ZPL is lowered by a small extent. If

the degree of the lowering of the ZPL in the upper electronic state is greater than that of the lower one, it causes a red shift in the transition energy. Oppositely, it yields a blue shift.

Table 5 lists the measured E_1 's and IEs of *o*-methoxyaniline, *m*-methoxyaniline, and *p*-methoxyaniline, and several substituted anilines [16,19,20,25–29]. These species have a general formula of $\text{XC}_6\text{H}_4\text{NH}_2$, where X is H, OH, OCH_3 , CH_3 , or F at the *ortho*, *meta*, or *para* position with respect to the NH_2 group. In consideration of the conductive effect, the OH, OCH_3 and CH_3 are classified as electron-donating groups whereas the F atom is an electron-withdrawing substituent. Previous R2PI and MATI experimental studies [25,26] show that the $\text{S}_1 \leftarrow \text{S}_0$ excitation mainly occurs around the ring whereas the transition from the S_1 to the D_0 state corresponds to the removal of one of the lone-pair electrons of nitrogen. Huang and Lombardi [30] performed Stark effect measurements and showed that *para* substituted anilines in the S_1 state can be viewed as a quinoid-like (dipolar) resonance structure, resulting from the dominant resonance effect. When the OH, OCH_3 , CH_3 , or F locate at the *para* position, they lead to a red shift in the E_1 due to the enhanced interaction between the substituents and the ring, as seen in Table 5. As for the *ortho* and *meta* positions, the observed shift in the E_1 results from the collective effect of the conductive and resonance factors.

As stated previously, the $\text{D}_0 \leftarrow \text{S}_1$ transition process involves the removal of one of the lone-pair electrons of the nitrogen or oxygen atoms of the substituents of aniline derivatives. Because the OH, OCH_3 and CH_3 can increase the electron density nearby the atom with lone-pair electrons, the $\text{D}_0 \leftarrow \text{S}_1$ transition energies (E_2 's) of aminophenol,

methoxyaniline, and methylaniline are lower than that of aniline. In contrast, the F atom can decrease the electron density and give rise to a higher E_2 for fluoroaniline. As the ionization process includes both $\text{S}_1 \leftarrow \text{S}_0$ and $\text{D}_0 \leftarrow \text{S}_1$ transitions, the IE is red-shifted for X = OH, OCH_3 and CH_3 and is blue-shifted for X = F, as seen in Table 5. In addition, the IEs of these *o*-, *m*-, *p*-substituted anilines follow the order: *para* < *ortho* < *meta*. These results suggest that both the nature and relative location of substituents can influence the adiabatic ionization energy.

5. Conclusion

We have applied the R2PI and MATI techniques to record the vibrational spectra of *m*-methoxyaniline and *o*-methoxyaniline in the S_1 and D_0 states. Analysis of these new data shows that the E_1 and adiabatic IE of *cis* *m*-methoxyaniline are determined to be 34308 ± 2 and $59983 \pm 5 \text{ cm}^{-1}$, whereas those of its *trans* rotamer are 34495 ± 2 and $60879 \pm 5 \text{ cm}^{-1}$, respectively. Most of the observed active vibrations of these isomeric species are related to the in-plane ring deformations. The frequencies of vibrations 6_{a} and 1 are measured to be 465 and 706 cm^{-1} for the *cis* and 468 and 709 cm^{-1} for the *trans* rotamer in the S_1 state; 537 and 726 cm^{-1} for the *cis* and 507 and 724 cm^{-1} for the *trans* rotamer in the D_0 state, respectively. This indicates that the molecular geometry is less rigid in the S_1 state than that in the D_0 state. In addition, different orientation of the OCH_3 group with respect to the NH_2 group as well as the electronic structures can influence the degree of both substituents involved in overall motion.

Similar to the cases of *o*-fluorophenol and *o*-methoxyphenol, only one stable structure of *o*-methoxyaniline is

Table 5
Measured electronic transition and ionization energies (in cm^{-1}) of substituted anilines

Molecule	$\text{S}_1 \leftarrow \text{S}_0$	ΔE_1	$\text{D}_0 \leftarrow \text{S}_1$	ΔE_2	IE	ΔIE
Aniline ^a	34029	0	28242	0	62271	0
<i>o</i> -Methoxyaniline ^b	33875	−154	24803	−3439	58678	−3593
<i>m</i> -Methoxyaniline, <i>cis</i> ^b	34308	279	25675	−2567	59983	−2288
<i>m</i> -Methoxyaniline, <i>trans</i> ^b	34495	466	26384	−1858	60879	−1392
<i>p</i> -Methoxyaniline ^c	31581	−2448	25864	−2378	57445	−4826
<i>m</i> -Aminophenol, <i>cis</i> ^d	34110	81	27350	−892	61460	−811
<i>m</i> -Aminophenol, <i>trans</i> ^d	34468	439	27266	−976	61734	−537
<i>p</i> -Aminophenol ^c	31393	−2636	27429	−813	58822	−3449
<i>o</i> -Methylaniline ^f	34318	289	26684	−1588	61002	−1269
<i>m</i> -Methylaniline ^f	33832	−197	27227	−1015	61059	−1212
<i>p</i> -Methylaniline ^f	33084	−945	27076	−1166	60160	−2111
<i>o</i> -Fluoroaniline ^g	34583	554	29061	819	63644	1373
<i>m</i> -Fluoroaniline ^h	34614	585	29545	1303	64159	1888
<i>p</i> -Fluoroaniline ^a	32652	−1377	29891	1649	62543	272

^a Refs. [25,26].

^b This work.

^c Ref. [16].

^d Refs. [18,19].

^e Refs. [18,20].

^f Ref. [27].

^g Ref. [28].

^h Refs. [28,29].

found. The E_1 and IE of *o*-methoxyaniline are measured to be 33875 ± 2 and $58678 \pm 5 \text{ cm}^{-1}$, respectively. Comparison of the experimental data shows that the E_1 's and IEs of *o*-, *m*-, and *p*-methoxyanilines follow the order: *para* < *ortho* < *meta*. The relatively low electronic transition and ionization energy of the *para* structural isomer may be attributed to the formation of the quinoid-like structure in the S_1 and D_0 states.

Acknowledgments

We gratefully thank the National Science Council of the Republic of China for financial support of this work under Grant No. NSC-95-2113-M-001-042-MY3.

References

- [1] J. Laane, Annu. Rev. Phys. Chem. 45 (1994) 179.
- [2] M. Thanneermalai, T. Jeyaraman, C. Sivakumar, A. Gopalan, T. Vasudevan, T.C. Wen, Spectrochim. Acta A 59 (2003) 1937.
- [3] P. Brown, Org. Mass Spectrom. 4 (1970) 519.
- [4] M. Shinozaki, M. Sakai, S. Yamaguchi, T. Fujioka, M. Fujii, Phys. Chem. Chem. Phys. 5 (2003) 5044.
- [5] S. Ullrich, W.D. Geppert, C.E.H. Dessent, K. Müller-Dethlefs, J. Phys. Chem. A 104 (2000) 11864.
- [6] N. Biswas, S. Wategaonkar, T. Watanabe, T. Ebata, N. Mikami, Chem. Phys. Lett. 394 (2004) 61.
- [7] J.L. Lin, L.C.L. Huang, W.B. Tzeng, J. Phys. Chem. A 105 (2001) 11455.
- [8] H. Dickinson, T. Chelmick, T.P. Softley, Chem. Phys. Lett. 338 (2001) 37.
- [9] S.J. Baek, K.W. Choi, Y.S. Choi, S.K. Kim, ~~J. Phys. Chem. A 109 (2003) 9487~~.
- [10] Th.L. Grebner, H.J. Neusser, Int. J. Mass Spectrom. Ion Proc. 159 (1996) 137.
- [11] J. Lin, W.B. Tzeng, Appl. Spectrosc. 57 (2003) 1178.
- [12] M. Gerhards, S. Schumm, C. Unterberg, K. Kleinermanns, Chem. Phys. Lett. 294 (1998) 65.
- [13] L. Yuan, C. Li, J.L. Lin, S.C. Yang, W.B. Tzeng, Chem. Phys. Lett. 323 (2006) 429.
- [14] P.G. Farrell, J. Newton, Tetrahedron Lett. (1966) 5517.
- [15] S. Wategaonkar, S. Doraiswamy, J. Chem. Phys. 106 (1997) 4894.
- [16] J. Lin, J.L. Lin, W.B. Tzeng, Chem. Phys. Lett. 370 (2003) 44.
- [17] M.J. Frisch, et al. GAUSSIAN 03, Revision C.02, Gaussian, Inc., Pittsburgh, 2003.
- [18] C. Uterberg, A. Gerlach, A. Jansen, M. Gerhards, Chem. Phys. 304 (2004) 237.
- [19] Y. Xie, H. Su, W.B. Tzeng, Chem. Phys. Lett. 394 (2004) 182.
- [20] Y. Xie, J.L. Lin, W.B. Tzeng, Chem. Phys. 305 (2004) 285.
- [21] J. Huang, J.L. Lin, W.B. Tzeng, ~~Chem. Phys. Lett., in press~~.
- [22] G. Varsanyi, Assignments of Vibrational Spectra of Seven Hundred Benzene Derivatives, Wiley, New York, 1974.
- [23] J. Huang, C. Li, W.B. Tzeng, Chem. Phys. Lett. 414 (2005) 276.
- [24] A.G. Csaszar, G. Fogarasi, Spectrochim. Acta A 45 (1989) 845.
- [25] X. Song, M. Yang, E.R. Davidson, J.P. Reilly, J. Chem. Phys. 99 (1993) 3224.
- [26] J. Lin, W.B. Tzeng, J. Chem. Phys. 115 (2001) 743.
- [27] J. Lin, K.C. Lin, W.B. Tzeng, J. Phys. Chem. A 106 (2002) 6462.
- [28] J. Lin, W.B. Tzeng, Phys. Chem. Chem. Phys. 2 (2000) 3759.
- [29] J. Lin, K.C. Lin, W.B. Tzeng, Appl. Spectrosc. 55 (2001) 120.
- [30] K.T. Huang, J.R. Lombardi, J. Chem. Phys. 51 (1969) 1228.